



Thermal energy storage properties and thermal reliability of PEG/bone char composite as a form-stable phase change material

Ruilong Wen^{1,3} · Puqi Jia^{2,3} · Zhaohui Huang¹ · Minghao Fang¹ · Yangai Liu¹ · Xiaowen Wu¹ · Xin Min¹ · Wei Gao³

Received: 3 September 2017 / Accepted: 15 December 2017 / Published online: 9 February 2018
© Akadémiai Kiadó, Budapest, Hungary 2018

Abstract

Bone char (BC) is a promising porous material that can be used for preparing a form-stable composite phase change material (PCM). In this paper, form-stable polyethylene glycol (PEG 6000)/BC composite PCMs were prepared by impregnation method. The PEG was used as the phase change material, and two different particle sizes of BC (0.8–1 mm: BC-1; 0.25–0.8 mm: BC-2) were acted as the supporting materials. The phase composition and chemical structure of the composite PCMs (PEG/BC-1 and PEG/BC-2) were characterized using X-ray diffraction and Fourier transformation infrared. The results indicated that the PEG can be well impregnated into BC pores with good compatibility. Thermal properties and thermal stability of the composite PCMs were determined by differential scanning calorimeter (DSC) and thermogravimetry analysis (TGA). DSC results showed that the maximum impregnation percentage for PEG into BC-1 and BC-2 was 38.77 and 43.91%, respectively, without melted PCM seepage from the composites. The TGA analysis revealed that the composite PCMs had good thermal stability above their working temperature range. The thermal cycle test of 100 melting–freezing cycles showed that the composite PCMs have good thermal reliability and chemical stability. The form-stable composite PCMs can be used as thermal energy storage material for waste heat storage and solar heating system.

Keywords Bone char · PEG · Form-stable composite PCM · Thermal energy storage

Introduction

The shortage of fossil energy and low energy efficiency has become the main limitation for the economy development of the world [1]. Research in renewable and clean energy

resource such as solar energy has been of vital importance [2]. Thermal energy storage has been proved to be an efficient technology for energy conservation which contains sensitive heat storage and latent heat storage. Latent heat storage using phase change materials (PCMs) is a promising way to increase the energy efficiency through

✉ Zhaohui Huang
huang118@cugb.edu.cn

✉ Wei Gao
w.gao@auckland.ac.nz

Ruilong Wen
wenruilong123@126.com

Puqi Jia
PuqiJia1988@hotmail.com

Minghao Fang
fmh@cugb.edu.cn

Yangai Liu
liuyang@cugb.edu.cn

Xiaowen Wu
xwwu@cugb.edu.cn

Xin Min
minxin4686@126.com

¹ Beijing Key Laboratory of Materials Utilization of Nonmetallic Minerals and Solid Wastes, National Laboratory of Mineral Materials, School of Materials Science and Technology, China University of Geosciences (Beijing), Beijing 100083, China

² Department of Nonferrous Metallurgy, School of Metallurgy, Northeastern University, 3 Wenhua Road, Shenyang 110819, China

³ Department of Chemical and Materials Engineering, The University of Auckland, Auckland, New Zealand

absorbing the industrial waste heat, solar thermal energy and environmental heat [3, 4]. In recent years, PCM has been developed for various applications such as thermal regulation of buildings [5, 6], electronic cooling [7], solar thermal systems [8–10] and food preservation [11].

According to the phase change type, PCM can be classified into four groups: solid–solid, solid–liquid, solid–gas and liquid–gas. Among these groups, the PCM with solid–liquid transitions is particularly valuable because of its advantages of high-energy storage density and small volume change during the phase change [12]. A large number of solid–liquid PCMs have been widely studied such as paraffin [13, 14], polyhydric alcohols [9], organic acid [15] and eutectic salt [16]. Polyethylene glycol (PEG) acting as a solid–liquid PCM has attracted more interest due to its suitable phase change temperature, high-energy storage density, nontoxicity and good thermal reliability [17, 18]. However, leakage during the melting process is a problem. Thus, the shape-stabilized PCM composed with supporting material and phase change material is needed to maintain the solid form even when the temperature is higher than the melting point of PCM [19, 20]. This means that the PCM does not leak and react with the surrounding material and environment.

Impregnating the PCM into porous materials has been studied [21–24]. Bone char (BC) is a porous adsorbent which can be obtained from carbonization of animal bones. Animal bone is a waste material that can be used to produce bone char by thermal treatment. It possesses highly porous structure and excellent absorption capacity [25, 26] and has been used in sewage disposal and drinking water purification [27]. Bone char has also been used for absorption of lead [28], fluoride [29] and arsenic [30] to clean the polluted water, but not been used to make composite PCM.

In this paper, a new novel composite phase change material was prepared by impregnation method. The PEG was chosen as the PCM, and two different sized bone char (0.8–1 mm: BC-1; 0.25–0.8 mm: BC-2) were used as the supporting material. The characterization and properties of the composites were determined. The results indicated that the PEG/BC composited PCM will be a potential candidate for waste heat storage and solar thermal energy storage systems.

Experimental

Materials

Cattle bones were used to make bone char. PEG 6000 was purchased from Interchem Agencies Ltd. Deionized water was used throughout the experimental process.

Preparation of bone char

The raw cattle bones were cut into small pieces (volume, 8–10 cm³), and was treated with boiled deionized water to remove the remaining protein and fat. The cleaned bones were grinded and sieved into different size (0.8–1 and 0.25–0.8 mm) followed by carburizing in a furnace at 200 °C for 2 h [31]. The schematic of experimental process is shown in Fig. 1a.

Preparation of form-stable composite PCMs

The form-stable composite PEG/BC was prepared by directly impregnation method [32, 33], Fig. 1b. PEG was put into a beaker and heated at 80 °C with magnetic stirring. Hot ethanol (80 °C) was then added into the beaker with melted PEG by the mass ratio of 1:1. BC with the mass ratio of PEG/BC = 150/100 was added into the beaker. The mixtures were magnetically stirred for 30 min to obtain composite PCMs, followed by drying on filter papers in an oven at 80 °C.

Characterization of form-stable composite PCMs

The pore volume, pore size and surface area of BC-1 were analyzed by Brunauer–Emmett–Teller method (BET, 3 Flex). The results are shown in Table 1. The chemical stability of the composite PCMs was determined by X-ray diffraction (XRD, Bruker D2 phaser) and FT-IR spectrometer (IRAffinity-1 Shimadzu). The XRD scanning range was from 10 to 80 °C. The infrared spectrum was measured in the range of 400–4000 cm⁻¹ with a resolution of 4 cm⁻¹ and the averaging over 30 scans.

Differential scanning calorimeter (DSC-60) was used to analysis the thermal properties of PCMs. A small amount of PCM sample was placed in an Al pan with cover lid and subjected to the DSC furnace. The parameters were set at a heat rate of 1 °C min⁻¹. The accuracy of temperature and enthalpy measurements was ± 1 °C and ± 2 J g⁻¹. Before testing the thermal properties, the DSC equipment was first calibrated which used the octadecane with thermal enthalpy of 240 J g⁻¹ as the energy calibration object and used water, In and Zn (melting point: 0 °C, 156.5 °C and 419.5 °C) as the temperature calibration object. The thermal stability of PCM was defined by thermogravimetric analysis (TGA, Shimadzu TGA-50) and derivative thermogravimetry (DTG). The heating rate was set as 10 °C min⁻¹ in the temperature range of 30–600 °C. The weight of TGA instrument was calibrated using the standard weight before it was used. A thermal cycle test involving 100 consecutive melting and solidifying cycles was proceeded to verify the thermal reliability. After

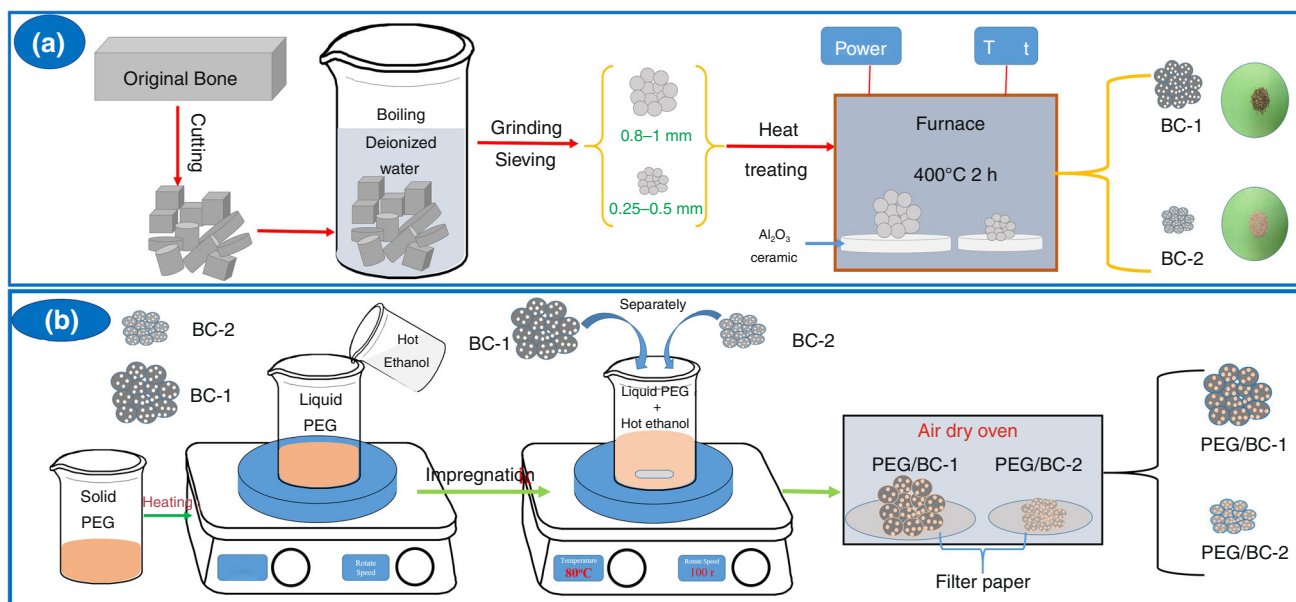


Fig. 1 **a** Schematic for the preparation of bone char and **b** schematic for the preparation of composite PCMs

Table 1 Surface area, pore volume and pore size of BC-1 and BC-2

Samples	Surface area/m ² g ⁻¹	Pore volume/mm ³ g ⁻¹	Pore size/nm
BC-1	112.551	2.858	13.5
BC-2	116.643	2.997	12.2

thermal cycling, the chemical and thermal properties of composite PCMs were determined by FT-IR and DSC.

Results and discussions

Characterization of composite phase change material

The textural properties of BC-1 and BC-2 are shown in Table 1. It can be seen that the pore volume of BC-1 and BC-2 was 2.858 and 2.997 mm³ g⁻¹ with the pore size of 13.5 and 12.2 nm, respectively. The surface area of BC-1 and BC-2 was 112.551 and 116.643 m² g⁻¹, respectively, which proves that the BC-1 and BC-2 have a good potential as the PCM supporting material.

The chemical compatibility of the components of the composite was characterized by evaluating the phase and chemical bond between PEG and BC using XRD and FT-IR technique. Figure 2 shows the XRD patterns of PEG, BC-1, BC-2 and composite PEG/BC-1, PEG/BC-2. While PEG has significant peaks at 19° and 23°, BC-1 and BC-2 possess the same diffraction peaks, indicating that they have the same phases. The XRD patterns of BC-1 and BC-2 show a poorly crystalline phase, possibly due to the existing of organic substances [34]. The main phase of BC-1 and BC-2 was hydroxyapatite with the characterize

peaks of 26.27°, 32.29°, 40.25°, 47.06°, 49.89° and 53.43°. It can also be seen that all sharp and intensive diffractions of PEG are observed in the PEG/BC-1 and PEG/BC-2 composite PCMs, indicating that the crystal structure of PEG is not destroyed after impregnation. All the other peaks correspond to BC-1 and BC-2, and no new peaks are

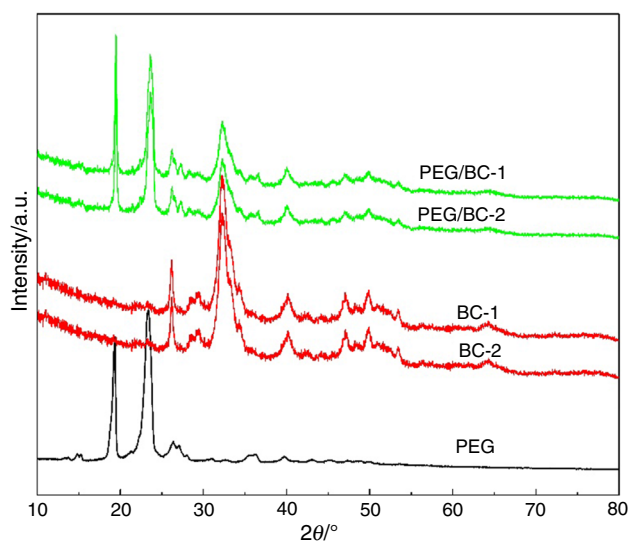


Fig. 2 XRD patterns of PEG, BC-1, BC-2 and composite PCMs (PEG/BC-1, PEG/BC-2)

observed; evidence of PEG and PEG-1 or PEG-2 is highly chemical compatible.

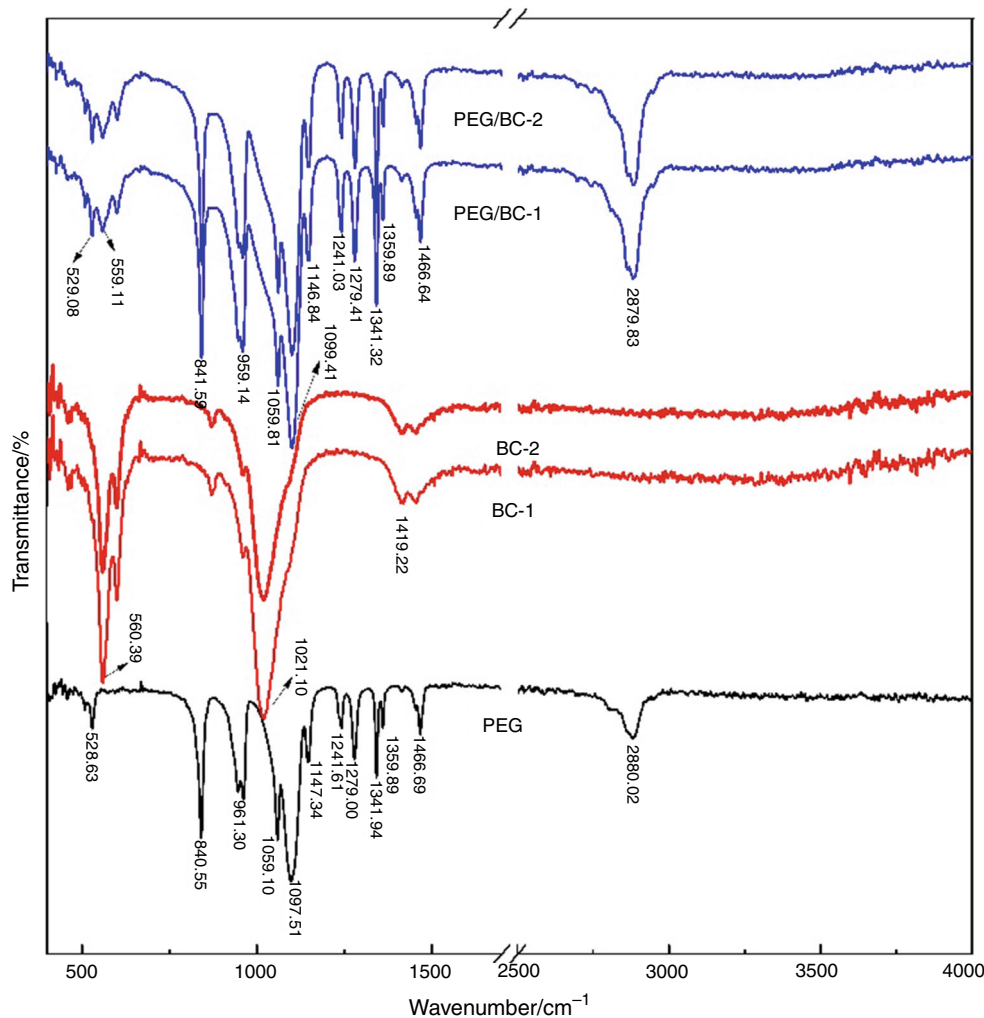
Figure 3 shows the FT-IR spectrum of PEG, BC-1, BC-2 and the composite PEG/BC-1, PEG/BC-2, indicating that the pure PEG has the characteristic peaks at 961.30, 1097.51, 1279.00, 1359.89, 1466.69 and 2880.02 cm^{-1} . The peak at 1097.51 cm^{-1} is attributed to the stretching vibration of the functional group of C–O. The peaks at 2880.02 and 961.30 cm^{-1} come from the stretching vibration of $-\text{CH}_2$ of PEG. The BC-1 and BC-2 bands at 603.11 and 1021.10 cm^{-1} can be attributed to the molecular vibration of PO_4^{3-} , similar to the FT-IR of camel bone charcoal [35]. The band at 1419.22 cm^{-1} is attributed to the stretching vibration for C–O bonds of carboxyl groups [36]. Finally, the band at 560.39 cm^{-1} corresponded to the calcium present in the organic structure, which is attributed to the bond between calcium and phosphate group [37, 38]. The PEG/BC-1 and PEG/BC-2 have the same FT-IR spectrums, which contain all characteristic peaks of PEG

and BC without significant new peak, evidence of no chemical interaction between PEG and BC.

Thermal properties of composite phase change materials

Figure 4 shows the DSC curves of the PEG, PEG/BC-1 and PEG/BC-2, with thermal properties listed in Table 2. It can be seen that the melting and freezing temperatures are, respectively, at 59.87 and 45.56 $^{\circ}\text{C}$ for PEG, 58.51 and 43.02 $^{\circ}\text{C}$ for PEG/BC-1, and 58.36 and 42.36 $^{\circ}\text{C}$ for PEG/BC-2. Compared with PEG, the phase change temperatures of PEG/BC-1 and PEG/BC-2 have changed a little probably due to the physical interaction implied in the FT-IR analysis [39]. However, Figure. 4a shows that each melting peak exhibited one shoulder on its increasing part, which may be attributed to the melting of polymer's one folded chains preceding that of the linear chains as previously underlined by Kovacs and Conthier [40]. Reversely, the composite PCMs show the bimodal crystallization behavior

Fig. 3 FT-IR spectrum of the PEG, BC-1, BC-2 and composite PCMs (PEG/BC-1, PEG/BC-2)



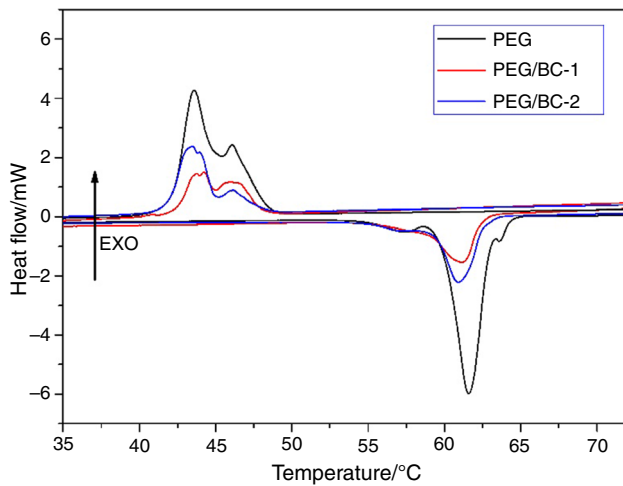


Fig. 4 DSC curves of the PEG, PEG/BC-1 and PEG/BC-2

on its freezing thermogram which probably due to the freezing temperature of the open-folded chains was a little different with the original PEG chains.

The latent heat of melting and freezing is 162.07 and 161.32 J g⁻¹ for PEG. The latent heat of composite PEG/BC-1 and PEG/BC-2 largely depends on the absorbed amounts of PEG. Table 1 lists the latent heat of melting and freezing of 62.67 and 59.93 J g⁻¹ for PEG/BC-1 and 71.17 and 68.43 J g⁻¹ for PEG/BC-2. Compared with the latent heat of PEG/BC-1, PEG/BC-1 with pure PEG, the PEG mass percentage in the composites can be determined from Eq. (1). The η represents the mass percentage of PCM in the composite. ΔH_{CPCM} is the melting latent heat of composite PCMs (PEG/BC-1 and PEG/BC-2), and ΔH_{PEG} is the melting latent heat of PEG measured by DSC. The calculated results are listed in Table 3.

$$\eta = \frac{\Delta H_{CPCM}}{\Delta H_{PEG}} \times 100\% \quad (1)$$

Other important parameters include impregnation efficiency (δ) and thermal storage capacity (σ), which are calculated by the following equations to characterize the thermal properties of composite PCMs (PEG/BC-1 and PEG/BC-2) [41].

$$\delta = \frac{\Delta H_{M-CPCM} + \Delta H_{F-CPCM}}{\Delta H_{M-PCM} + \Delta H_{F-PCM}} \times 100\% \quad (2)$$

$$\sigma = \frac{\frac{\Delta H_{M-CPCM} + \Delta H_{F-CPCM}}{\eta}}{\Delta H_{M-PCM} + \Delta H_{F-PCM}} \times 100\% \quad (3)$$

where H_{M-CPCM} and H_{M-PCM} are the melting and freezing enthalpy of PEG/BC-1 and PEG/BC-2. H_{M-CPCM} and H_{M-PCM} are the melting and freezing enthalpy of pure PEG. The calculated value of δ and σ are listed in Table 3. The impregnation efficiency represents the effective latent heat storage of PEG inside the BC porous structure. As we can see, the sample PEG/BC-1 and PEG/BC-2 achieved the impregnation efficiency of 37.91 and 43.17% when the maximum PCM percentages reach to 38.67 and 43.91%, respectively. It is also found that PEG/BC-1 and PEG/BC-2 have the thermal storage capacity of 98.03 and 98.31%, indicating that almost all impregnation PEG can store thermal energy through phase change.

Leakage analysis of composite phase change materials

The leakage of composite PCMs of PEG/BC-1 and PEG/BC-2 would limit its application. Figure 5 shows the leakage results of pure PEG and composite PCMs. As seen in Fig. 5, the pure PEG melted after heat treated at 80 °C for 1 min, but the shape of PEG/BC-1 and PEG/BC-2 has no change after heat treated at 80 °C for 30 min, and the filter paper also has no trace of leakage. These results reveal that there were no leakage in phase change process of PEG/BC-1 and PEG/BC-2.

Thermal stability of the composite phase change materials

TGA curves are shown in Fig. 6a, b to assess the thermal stability of PEG, BC-1, BC-2, PEG/BC-1 and PEG/BC-2. The corresponding DTG curves are shown in Fig. 7. The mass of BC-1 and BC-2 decreased during TGA test due to the loss of water and activated carbon in the porous and crystal BC. Therefore, the actual mass of PEG in the BC-1 and BC-2 can be calculated by Eq. (4), where φ is the

Table 2 DSC data of PEG and composite PCMs

Samples	(Before thermal cycles)		(After thermal cycles)		(Before thermal cycles)		(After thermal cycles)	
	Temperature/°C	Latent heat/J g ⁻¹	Temperature/°C	Latent heat/J g ⁻¹	Temperature/°C	Latent heat J g ⁻¹	Temperature/°C	Latent heat/J g ⁻¹
PEG	59.87	162.07	—	—	45.56	161.32	—	—
PEG + BC-1	58.51	62.67	58.14	61.33	43.02	59.93	42.76	60.04
PEG + BC-2	59.36	71.17	59.04	71.03	42.36	68.43	44.03	71.16

Table 3 Thermal characteristic of composite PCMs

Samples	PCM percentage $\eta/\%$	Impregnation efficiency $\delta/\%$	Thermal storage capacity $\sigma/\%$
PEG/BC-1	38.67	37.91	98.03
PEG/BC-2	43.91	43.17	98.31

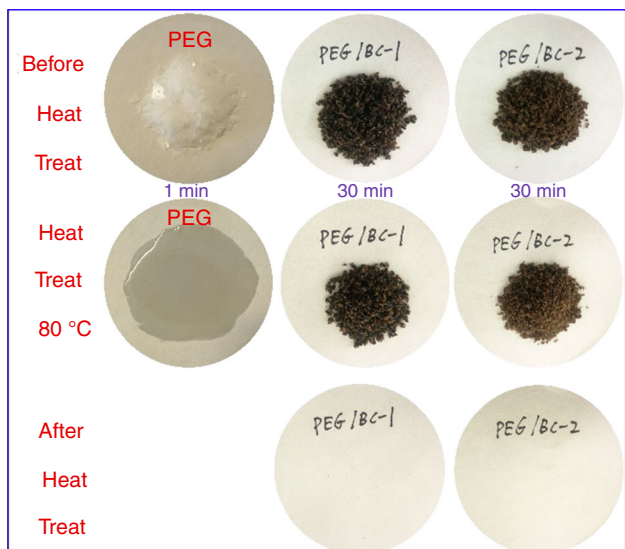


Fig. 5 Leakage test of composite phase change materials

actual mass percentage of PEG in the BC-1 and BC-2; *a*, *b* and *c*, respectively, represent the weight losses of pure PEG, BC (BC-1 and BC-2) and PEG/BC when temperature reached 460 °C.

$$\varphi = \frac{c - b}{a - b} \tag{4}$$

The actual mass percentage of PEG in BC-1 and BC-2 was 46.39 and 46.09% which was higher than the value

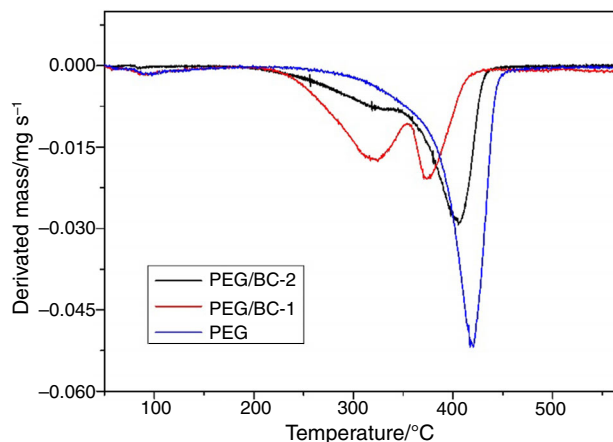


Fig. 7 DTA curves of PEG, PEG/BC-1 and PEG/BC-2

calculated by the thermal enthalpy, implying that not all PEG in the porous of BC act as PCM.

As seen from Fig. 7, the pure PEG exhibits a degradation step with the peak at 423.5 °C. PEG/BC-1 and PEG/BC-2 display a two-step thermal degradation process due to the different heat transfer rate in the porous of BC [42]. However, the beginning degradation temperature of PEG/BC-1 and PEG/BC-2 was 274.5 and 382.5 °C, indicating that PEG/BC-1 and PEG/BC-2 have a good thermal stability under 250 °C, especially for PEG/BC-2. Accordingly, PEG/BC-1 and PEG/BC-2 have potential applications in solar energy storage and energy efficiency buildings.

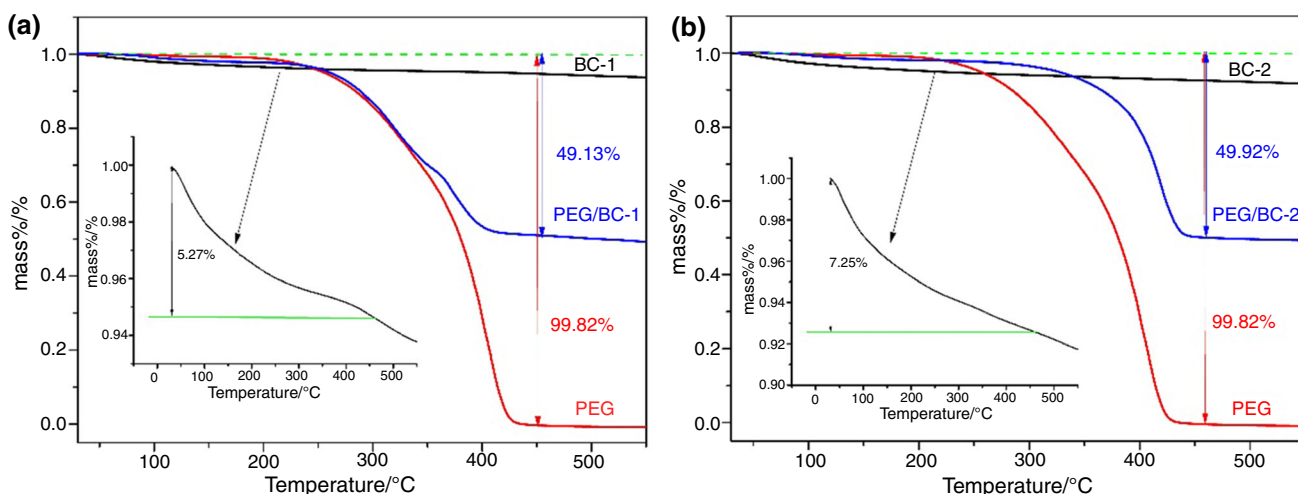


Fig. 6 TGA curves of **a** PEG, BC-1 and PEG/BC-1; **b** PEG, BC-2 and PEG/BC-2

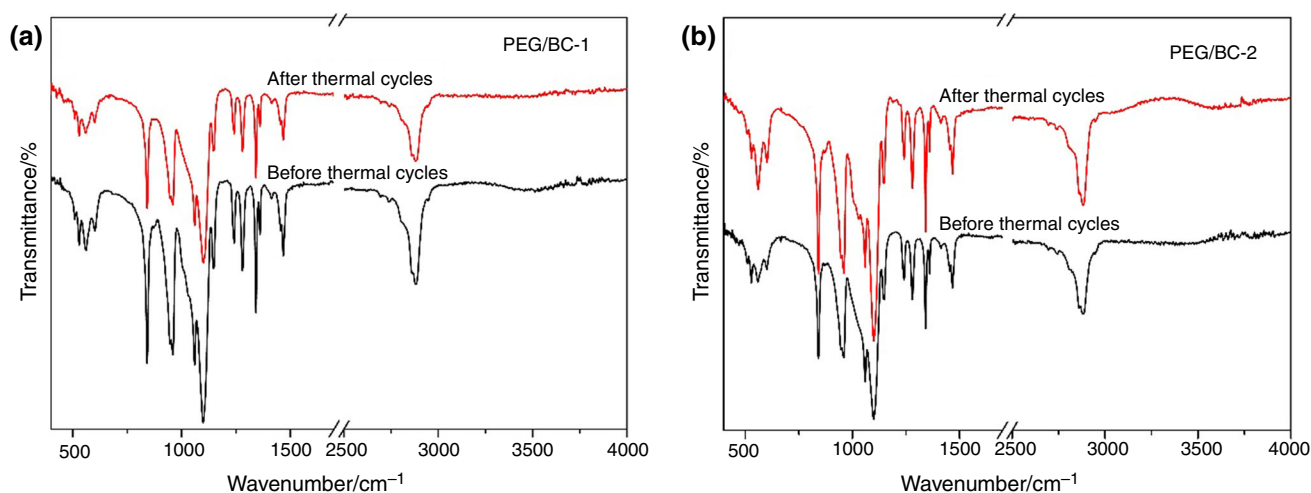


Fig. 8 FT-IR spectra of **a** PEG/BC-1 and **b** PEG/BC-2 before and after 100 thermal cycles

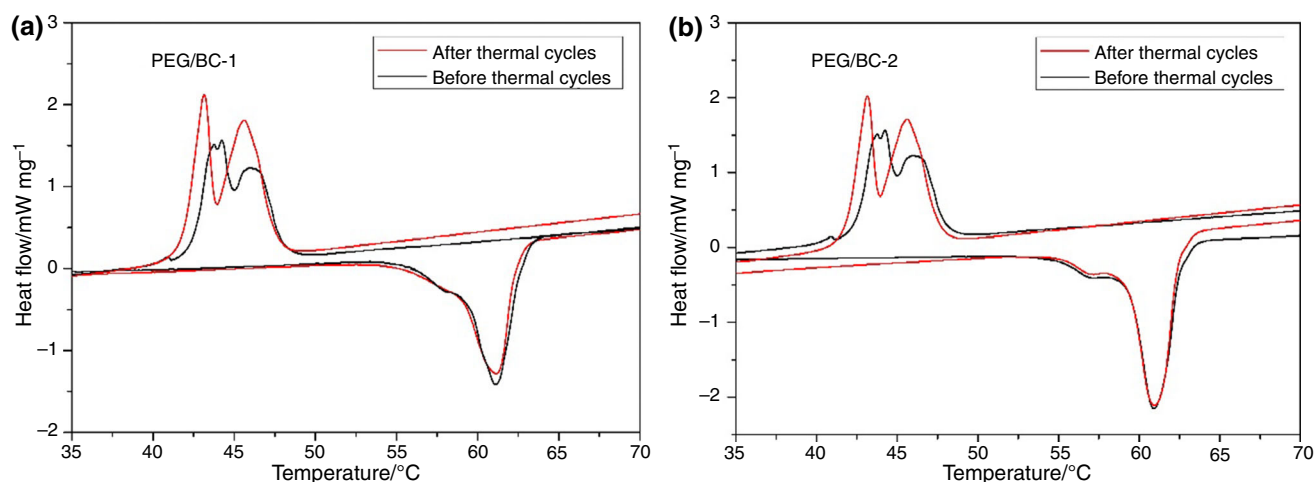


Fig. 9 DSC curves of **a** PEG/BC-1 and **b** PEG/BC-2 before and after thermal cycles

Thermal reliability of form-stable composite PCMs

The composite PCM must be stable in terms of chemical and thermal manner after melting and freezing thermal cycles. Therefore, thermal cycles test was carried out to determine the change in chemical structure and thermal properties. Figure 8 shows the FT-IR spectrum of PEG/BC-1 and PEG/BC-2 before and after thermal cycles. As seen from the spectrum, the shape and position of all peaks of PEG/BC-1 and PEG/BC-2 have no change after 100 thermal cycles, indicating that the chemical structure of composite PCMs has not been affected by melting and freezing cycles.

Figure 9 shows the DSC curves of PEG/BC-1 and PEG/BC-2 before and after thermal cycles with data listed in Table 2. The melting and freezing temperatures of PEG/BC-1 have only changed by -0.37 and -0.26 °C after

100 thermal cycles, while the melting and freezing enthalpy changed by -1.34 and 0.11 J g⁻¹. For PEG/BC-2, the melting and freezing temperatures have changed by 0.72 and -0.58 °C, and the enthalpy changed by -0.14 and -0.22 J g⁻¹. The changes in thermal properties are at a reasonable level for energy storage applications. It can also be seen that the freezing behavior has changed apparently after thermal cycles, which may be caused by the position change of PEG impregnated in BC and the different positions in BC have different thermal transfer rates [42].

Conclusions

Two different sized bone char (0.8–1 and 0.25–0.8 mm) were used as the supporting materials to prepare composite PCMs. PEG (PEG 6000) acts as the phase change material.

Two shape-stable composite PCMs were prepared by impregnate method. The maximum mass ratio of PEG into BC-1 and BC-2 is 38.67 and 43.91%, respectively. The form-stable composite PEG/BC-1 and PEG/BC-2 melt at 58.51 and 58.36 °C with latent heat of 62.67 and 71.17 J g⁻¹; and the freeze temperatures are 43.02 and 42.36 °C with latent heat of 59.93 and 68.43 J g⁻¹. The PEG/BC-1 and PEG/BC-2 PCMs possess good thermal stability especially PEG/BC-2 above their working temperature. Moreover, the chemical structure and thermal properties of these PCMs are well maintained after 100 thermal cycles. The results indicate that these form-stable composite has potential applications in solar thermal energy storage and energy efficient buildings.

Acknowledgements We gratefully acknowledge the China Scholarship Council (CSC) for providing the opportunity to study at the University of Auckland, and the assistance from the group and department. This present work was supported by the National Natural Science Foundations of China (Grant Nos. 51472222, 51372232).

References

- Cao L, Tang Y, Fang G. Preparation and properties of shape-stabilized phase change materials based on fatty acid eutectics and cellulose composites for thermal energy storage. *Energy*. 2015;80:98–103.
- Crabtree GW, Lewis NS. Solar energy conversion. *Phys Today*. 2007;60(3):37–42.
- Chen L, Zou R, Xia W, Liu Z, Shang Y, Zhu J, et al. Electro- and photodriven phase change composites based on wax-infiltrated carbon nanotube sponges. *ACS Nano*. 2012;6(12):10884–92.
- Fang G, Li H, Liu X. Preparation and properties of lauric acid/silicon dioxide composites as form-stable phase change materials for thermal energy storage. *Mater Chem Phys*. 2010;122(2–3):533–6.
- Dincer I. On thermal energy storage systems and applications in buildings. *Energy Build*. 2002;34(4):377–88.
- Tyagi VV, Buddhi D. PCM thermal storage in buildings: a state of art. *Renew Sustain Energy Rev*. 2007;11(6):1146–66.
- Kandasamy R, Wang X-Q, Mujumdar AS. Application of phase change materials in thermal management of electronics. *Appl Therm Eng*. 2007;27(17–18):2822–32.
- Cai Y, Gao C, Xu X, Fu Z, Fei X, Zhao Y, et al. Electrospun ultrafine composite fibers consisting of lauric acid and polyamide 6 as form-stable phase change materials for storage and retrieval of solar thermal energy. *Sol Energy Mater Sol Cells*. 2012;103:53–61.
- Karaman S, Karaipekli A, Sari A, Biçer A. Polyethylene glycol (PEG)/diatomite composite as a novel form-stable phase change material for thermal energy storage. *Sol Energy Mater Sol Cells*. 2011;95(7):1647–53.
- Qiu X, Song G, Chu X, Li X, Tang G. Microencapsulated n-alkane with p(n-butyl methacrylate-co-methacrylic acid) shell as phase change materials for thermal energy storage. *Sol Energy*. 2013;91:212–20.
- Gin B, Farid MM. The use of PCM panels to improve storage condition of frozen food. *J Food Eng*. 2010;100(2):372–6.
- Cao L, Tang F, Fang G. Synthesis and characterization of microencapsulated paraffin with titanium dioxide shell as shape-stabilized thermal energy storage materials in buildings. *Energy Build*. 2014;72:31–7.
- Rao ZH, Wang SH, Zhang YL, Zhang GQ, Zhang JY. Thermal properties of paraffin/nano-AlN phase change energy storage materials. *Energy Sour Part A Recovery Util Environ Eff*. 2014;36(20):2281–6.
- Silakhori M, Naghavi M, Metselaar H, Mahlia T, Fauzi H, Mehrali M. Accelerated thermal cycling test of microencapsulated paraffin wax/polyaniline made by simple preparation method for solar thermal energy storage. *Materials*. 2013;6(5):1608–20.
- Karaipekli A, Sari A. Capric–myristic acid/vermiculite composite as form-stable phase change material for thermal energy storage. *Sol Energy*. 2009;83(3):323–32.
- Jiang Y, Sun Y, Bruno F, Li S. Thermal stability of Na₂CO₃–Li₂CO₃ as a high temperature phase change material for thermal energy storage. *Thermochim Acta*. 2017;650:88–94.
- Qian T, Li J, Min X, Guan W, Deng Y, Ning L. Enhanced thermal conductivity of PEG/diatomite shape-stabilized phase change materials with Ag nanoparticles for thermal energy storage. *J Mater Chem A*. 2015;3(16):8526–36.
- Wang W, Yang X, Fang Y, Ding J. Preparation and performance of form-stable polyethylene glycol/silicon dioxide composites as solid–liquid phase change materials. *Appl Energy*. 2009;86(2):170–4.
- Cai Y, Sun G, Liu M, Zhang J, Wang Q, Wei Q. Fabrication and characterization of capric–lauric–palmitic acid/electrospun SiO₂ nanofibers composite as form-stable phase change material for thermal energy storage/retrieval. *Sol Energy*. 2015;118:87–95.
- Cao L, Tang F, Fang G. Preparation and characteristics of microencapsulated palmitic acid with TiO₂ shell as shape-stabilized thermal energy storage materials. *Sol Energy Mater Sol Cells*. 2014;123:183–8.
- Xu B, Li Z. Paraffin/diatomite composite phase change material incorporated cement-based composite for thermal energy storage. *Appl Energy*. 2013;105:229–37.
- Xia L, Zhang P, Wang RZ. Preparation and thermal characterization of expanded graphite/paraffin composite phase change material. *Carbon*. 2010;48(9):2538–48.
- Sari A, Karaipekli A, Alkan C. Preparation, characterization and thermal properties of lauric acid/expanded perlite as novel form-stable composite phase change material. *Chem Eng J*. 2009;155(3):899–904.
- Li M, Kao H, Wu Z, Tan J. Study on preparation and thermal property of binary fatty acid and the binary fatty acids/diatomite composite phase change materials. *Appl Energy*. 2011;88(5):1606–12.
- Tala W, Chantara S, Thiansem S, Rayanakorn M. Development of low-cost passive sampler from cow bone char for sampling of volatile organic compounds. *Int J Environ Sci Technol*. 2016;13(7):1685–96.
- Javad Assari M, Rezaee A, Rangkooy H. Bone char surface modification by nano-gold coating for elemental mercury vapor removal. *Appl Surf Sci*. 2015;342:106–11.
- Rezaee A, Ghanizadeh G, Behzadiyannejad G, Yazdambakhsh A, Siyadat SD. Adsorption of endotoxin from aqueous solution using bone char. *Bull Environ Contam Toxicol*. 2009;82(6):732–7.
- Chen SB, Zhu YG, Ma YB, McKay G. Effect of bone char application on Pb bioavailability in a Pb-contaminated soil. *Environ Pollut*. 2006;139(3):433–9.
- Medellin-Castillo NA, Leyva-Ramos R, Ocampo-Perez R, Garcia de la Cruz RF, Aragon-Piña A, Martinez-Rosales JM, et al. Adsorption of fluoride from water solution on bone char. *Ind Eng Chem Res*. 2007;46(26):9205–12.

30. Chen YN, Chai LY, Shu YD. Study of arsenic (V) adsorption on bone char from aqueous solution. *J Hazard Mater.* 2008;160(1):168–72.
31. Patel S, Han J, Qiu W, Gao W. Synthesis and characterisation of mesoporous bone char obtained by pyrolysis of animal bones, for environmental application. *J Environ Chem Eng.* 2015;3(4):2368–77.
32. Sari A, Karaipekli A. Fatty acid esters-based composite phase change materials for thermal energy storage in buildings. *Appl Therm Eng.* 2012;37:208–16.
33. Feldman D, Banu D, Hawes D, Ghanbari E. Obtaining an energy storing building material by direct incorporation of an organic phase change material in gypsum wallboard. *Sol Energy Mater.* 1991;22(2–3):231–42.
34. Figueiredo M, Fernando A, Martins G, Freitas J, Judas F, Figueiredo H. Effect of the calcination temperature on the composition and microstructure of hydroxyapatite derived from human and animal bone. *Ceram Int.* 2010;36(8):2383–93.
35. Hassan SS, Awwad NS, Aboterika AH. Removal of mercury (II) from wastewater using camel bone charcoal. *J Hazard Mater.* 2008;154(1–3):992–7.
36. Jiang Y, Wang B, Meng F, Cheng Y, Zhu C. Microwave-assisted preparation of N-doped carbon dots as a biosensor for electrochemical dopamine detection. *J Colloid Interface Sci.* 2015;452:199–202.
37. Lurtwitayaponta S, Srisatit T. Comparison of lead removal by various types of swine bone adsorbents. *Environ Asia.* 2010;3:32–8.
38. Varma HK, Suresh Babu S. Synthesis of calcium phosphate bioceramics by citrate gel pyrolysis method. *Ceram Int.* 2005;31(1):109–14.
39. Tang F, Cao L, Fang G. Preparation and thermal properties of stearic acid/titanium dioxide composites as shape-stabilized phase change materials for building thermal energy storage. *Energy Build.* 2014;80:352–7.
40. Khalil SA, Moustafa MA, Ebian AR, Motawi MM. GI absorption of two crystal forms of sulfameter in man. *J Pharm Sci.* 1972;61(10):1615–7.
41. Yu S, Wang X, Wu D. Microencapsulation of n-octadecane phase change material with calcium carbonate shell for enhancement of thermal conductivity and serving durability: synthesis, microstructure, and performance evaluation. *Appl Energy.* 2014;114:632–43.
42. Brown JM, Bemis WA. Bone char reactivation. *Ind Eng Chem.* 1940;32(8):1112–4.